



HAL
open science

Verifying robust output amplitude constraints for multisine excitation in system identification

Xavier Bombois, Gérard Scorletti, Guillaume Mercère

► **To cite this version:**

Xavier Bombois, Gérard Scorletti, Guillaume Mercère. Verifying robust output amplitude constraints for multisine excitation in system identification. 2024. hal-04675923v1

HAL Id: hal-04675923

<https://hal.science/hal-04675923v1>

Preprint submitted on 23 Aug 2024 (v1), last revised 15 Oct 2024 (v2)

HAL is a multi-disciplinary open access archive for the deposit and dissemination of scientific research documents, whether they are published or not. The documents may come from teaching and research institutions in France or abroad, or from public or private research centers.

L'archive ouverte pluridisciplinaire **HAL**, est destinée au dépôt et à la diffusion de documents scientifiques de niveau recherche, publiés ou non, émanant des établissements d'enseignement et de recherche français ou étrangers, des laboratoires publics ou privés.

Verifying robust output amplitude constraints for multisine excitation in system identification

X. Bombois ^{a,b} G. Scorletti ^a G. Mercère ^c

^aLaboratoire Ampère, Ecole Centrale de Lyon, Université de Lyon, 36 avenue Guy de Collongue, Ecully, France

^bCentre National de la Recherche Scientifique (CNRS), France

^cUniversité de Poitiers, LIAS, Poitiers, France

Abstract

In this paper, we consider the problem of system identification with output amplitude constraints for the case of a multisine excitation. The main contribution of the paper is to provide an LMI optimization problem to verify whether the output amplitude constraint is satisfied for all systems in an uncertainty region containing the unknown true system. In addition, input amplitude constraints can also be verified using the results of this paper.

Key words: Amplitude constraints, System identification, Robustness analysis

1 Introduction

In this paper, we consider system identification with a multisine excitation and we develop a methodology to verify whether a given multisine excitation respects input and output amplitude constraints. For this purpose, we make use of an uncertainty region for the unknown true system.

Besides a model \hat{G} of the unknown true system G_0 , prediction error identification [16] allows to derive an uncertainty region \mathcal{D} for G_0 . Different types of uncertainty regions have been considered in the literature. When the identification is performed in a full-order model structure, the obtained uncertainty region \mathcal{D} is a set of parametrized transfer functions $G(\theta)$ whose parameter vector θ is constrained to lie in an ellipsoid U in the parameter space [16,5]. When the model structure is not full-order, the obtained uncertainty region \mathcal{D} is a set of systems G whose frequency response is, at each frequency ω , constrained to lie in an ellipse $U(\omega)$ in the Nyquist plane [12,4,13,20].

With respect to the uncertainty regions that are generally considered in robustness analysis [22], the uncertainty regions \mathcal{D} delivered by system identification are rather non-standard. However, in the last twenty years, numerous robustness analysis tools have been developed for these types of uncertainty regions (mainly for the parametric uncertainty region). In [5,4,1], we have, e.g., developed an LMI optimization procedure to verify whether the worst-case H_∞ performance achieved by a

given controller over the plants in \mathcal{D} is acceptable. The case of the worst-case H_2 performance is treated in [6]. In [14], it is shown that more complex robust performance criteria can be addressed at the cost of a second-order Taylor approximation. Note that many of these robustness tools have been integrated into optimal experiment design schemes aiming at obtaining optimal models for control [8,1,6,14].

In relation with these developments around optimal experiment design, robust output power constraints have also been considered i.e., robustness analysis tools have been developed to verify whether a given excitation will not lead to an excessive output power during an identification experiment. Since the output obviously depends on the unknown true system G_0 , it is in fact verified whether the output for all systems $G \in \mathcal{D}$ has an acceptable power. The case of multisine excitation is treated in [7], while robust output power constraints for filtered white noise excitation can be addressed using the tools in [6].

In many applications though (see, e.g., [18] for an example), the constraints are not formulated as constraints on the power of the output signal, but as constraints on the amplitude of the time-domain sequence of this signal. As mentioned above, in this paper, we will therefore develop a methodology to handle robust output *amplitude* constraints. Since the (robust) output *amplitude* constraint can easily be translated into a (robust) output *power* constraint for filtered white

noise excitation, we will here only consider the case of multisine excitation. Such robust amplitude constraints could until now only be treated via an approximation of the uncertainty set \mathcal{D} i.e., the output constraint is only verified for a limited number of grid points in \mathcal{D} (see, e.g., [17]). In this paper, we use the robustness analysis philosophy to avoid the approximation of the uncertainty region \mathcal{D} and we develop an LMI optimization problem which allows, for a given multisine excitation, to verify whether the output amplitude constraint is satisfied for the outputs of all systems $G \in \mathcal{D}$. We do that for both types of uncertainty regions \mathcal{D} delivered by system identification. Since amplitude constraints must be respected at each time instant, we treat, in this LMI formulation, the time similarly as the systems $G \in \mathcal{D}$ i.e., as an uncertain variable varying in a set. Using the same philosophy, we also develop an LMI optimization problem to verify whether an *input* amplitude constraint is verified at each time instant.

Notations. Continuous-time signals will be denoted $x(t)$ where $t \in \mathbb{R}$ is the time index. The variable s is the Laplace variable while z will denote both the Z-transform variable and the shift operator. We use j to represent $\sqrt{-1}$. For a complex number a (i.e., $a \in \mathbb{C}$), $|a|$, $\angle a$, $Re(a)$, $Im(a)$ will denote, respectively, its modulus, its argument, its real part and its imaginary part. For a real number a (i.e., $a \in \mathbb{R}$), $|a|$ is the absolute value of a . For a matrix A , A^T (resp. A^*) is its transpose (resp. conjugate transpose). With some abuse, we will use 0 both for zero and for zero matrices. The matrix

$$\begin{pmatrix} X_1 & 0 & 0 \\ 0 & \ddots & 0 \\ 0 & 0 & X_n \end{pmatrix}$$

will be denoted $diag(X_1, \dots, X_n)$ if the elements X_i ($i = 1, \dots, n$) are scalar quantities, while it will be denoted $bdiag(X_1, \dots, X_n)$ if the elements X_i ($i = 1, \dots, n$) are matrices. In addition, I_n represents the identity matrix of dimension $n \times n$ and \otimes , the Kronecker product. The unit ball of dimension n is denoted \mathcal{B}_n i.e., $\mathcal{B}_n = \{\delta \in \mathbb{R}^n \mid \delta^T \delta \leq 1\}$. For two matrices Δ and

$$M = \left(\begin{array}{c|c} M_{11} & M_{12} \\ \hline M_{21} & M_{22} \end{array} \right) \text{ with } \Delta \in \mathbb{C}^{m \times n} \text{ and } M_{11} \in \mathbb{C}^{n \times m},$$

$\Delta \star M$ is given by $\Delta \star M \triangleq M_{22} + M_{21} \Delta (I_n - M_{11} \Delta)^{-1} M_{12}$ (the symbol \star stands thus here for the Redheffer product). Moreover, the relation $y = (\Delta \star M)u$ (with vectors y and u) can always be represented via internal vectors p and q in the following LFT expression:

$$p = \Delta q \text{ and } \begin{pmatrix} q \\ y \end{pmatrix} = \begin{pmatrix} M_{11} & M_{12} \\ M_{21} & M_{22} \end{pmatrix} \begin{pmatrix} p \\ u \end{pmatrix}.$$

2 Problem statement

We consider input-output amplitude constraints for the identification of a discrete-time model of a stable

single-input single-output true system which can be described by a continuous-time transfer function $G_0^c(s)$ with input u and output y . The discrete-time data for the identification of the discrete-time model of $G_0^c(s)$ will be gathered in open loop by sampling the continuous-time input-output signals at a rate T_s (after the application of an anti-aliasing filter). The obtained discrete-time model $\hat{G}(z)$ will therefore be an estimate of a discrete-time transfer function $G_0(z)$ which satisfies $G_0(e^{j\omega T_s}) = G_0^c(j\omega)$ for $\omega \in [0, \frac{\pi}{T_s}]$. We also suppose that we have an uncertainty region \mathcal{D} containing the true discrete-time system $G_0(z)$. This uncertainty region will typically originate from an initial identification experiment.

In order to, e.g., reduce this initial uncertainty, we wish to perform a second identification experiment using a multisine excitation i.e., the continuous-time true system $G_0^c(s)$ will be excited by a (continuous-time) multisine excitation signal having the general expression:

$$u(t) = \sum_{i=1}^L (a_{i,s} \sin(\omega_i t) + a_{i,c} \cos(\omega_i t)), \quad (1)$$

where $a_{i,s}$, $a_{i,c}$ (resp. ω_i) ($i = 1, \dots, L$) are user-chosen amplitudes (resp. frequencies). The fundamental frequency of this multisine will be denoted ω_0 . Each of the L frequencies ω_i ($i = 1, \dots, L$) thus satisfies the following relation:

$$\omega_i = \alpha_i \omega_0 \quad (2)$$

for an integer $\alpha_i \neq 0$ ($i = 1, \dots, L$). Since the discrete-time data will be gathered with a sampling rate T_s , we will suppose that $\omega_L < \frac{\pi}{T_s}$. For the sequel, it is important to notice that the multisine (1) can be equivalently written in the following phasor form:

$$u(t) = Re(\mathcal{A}^T \mathcal{U}(t)), \quad (3)$$

where $\mathcal{U}(t)$ and \mathcal{A} are complex column vectors of dimension L whose i^{th} entries are respectively given by $\mathcal{U}_i(t) = e^{j\omega_i t}$ and $\mathcal{A}_i = a_{i,c} - j a_{i,s}$ ($i = 1, \dots, L$). Using the same phasor notation and the fact that $G_0(e^{j\omega T_s}) = G_0^c(j\omega)$ for $\omega \in [0, \frac{\pi}{T_s}]$, the (noise-free) steady-state output of $G_0^c(s)$ under this multisine excitation is given by:

$$y(t, G_0) \triangleq Re(\mathcal{A}^T diag(G_0(e^{j\omega_1 T_s}), \dots, G_0(e^{j\omega_L T_s})) \mathcal{U}(t)). \quad (4)$$

Even though the frequency response of $G_0^c(s)$ could also have been used in (4), the discrete-time version $G_0(z)$ of $G_0^c(s)$ is used instead since it is this transfer function which lies in \mathcal{D} . Note that both $u(t)$ and $y(t, G_0)$ are periodic signals with period $T_0 = \frac{2\pi}{\omega_0}$. This will also be the case for the signal $y(t, G)$ obtained by replacing, in (4), $G_0(z)$ by a system $G(z) \in \mathcal{D}$. In the sequel, we will denote $T_P = [0, \frac{2\pi}{\omega_0}]$ the time interval corresponding to a period of these multisines.

In the sequel, we will suppose that we have the following input and output amplitude constraints:

$$\begin{aligned} -\bar{\mathbf{u}}_{\max} &\leq u(t) \leq \bar{\mathbf{u}}_{\max} \quad \forall t \in T_P \\ -\bar{\mathbf{y}}_{\max} &\leq y(t, G_0) \leq \bar{\mathbf{y}}_{\max} \quad \forall t \in T_P \end{aligned} \quad (5)$$

for some given thresholds $\bar{\mathbf{u}}_{\max} > 0$ and $\bar{\mathbf{y}}_{\max} > 0$. Note that the output amplitude constraint here pertains to the noise-free steady-state output $y(t, G_0)$. See Section 2 of [9] to see how to deal with the transient and with the noise corrupting the output.

In order to verify (5) before the application of the multisine $u(t)$ to the true system, we wish to evaluate the following quantities:

$$u_{wc} = \max_{t \in T_P} |u(t)|, \quad (6)$$

$$y_{wc} = \max_{t \in T_P} \max_{G(z) \in \mathcal{D}} |y(t, G)|, \quad (7)$$

with $y(t, G)$ defined in (4). The amplitude constraints will indeed be respected if $u_{wc} \leq \bar{\mathbf{u}}_{\max}$ and $y_{wc} \leq \bar{\mathbf{y}}_{\max}$ (since the unknown transfer function $G_0(z)$ lies in \mathcal{D}).

In order to be able to evaluate u_{wc} and y_{wc} in a tractable manner, we will introduce the following change of variable:

$$\tau \triangleq e^{j\omega_0 t}, \quad (8)$$

with ω_0 the fundamental frequency of $u(t)$. Using (2), we have $\mathcal{U}_i(t) = e^{j\omega_i t} = \tau^{\alpha_i}$ ($i = 1, \dots, L$). Consequently, introducing $\tilde{\mathcal{U}}(\tau) = (\tau^{\alpha_1}, \tau^{\alpha_2}, \dots, \tau^{\alpha_L})^T$, (6) and (7) can be equivalently rewritten as:

$$u_{wc} = \max_{\tau \in \mathcal{T}} |Re(x_u(\tau))| \quad \text{with } x_u(\tau) = \mathcal{A}^T \tilde{\mathcal{U}}(\tau) \quad (9)$$

$$y_{wc} = \max_{\tau \in \mathcal{T}} \max_{G \in \mathcal{D}} \left| Re \left(\mathcal{A}^T \text{diag}(G(e^{j\omega_1 T_s}), \dots, G(e^{j\omega_L T_s})) \tilde{\mathcal{U}}(\tau) \right) \right| \quad (10)$$

with

$$\mathcal{T} = \{\tau \in \mathbb{C} \mid \tau^* \tau = 1\}. \quad (11)$$

Observe that, in the same way as G is an uncertain system lying in \mathcal{D} , the variable τ can also be seen as an uncertain variable which lies in the set \mathcal{T} .

3 Uncertainty region \mathcal{D}

As indicated in the previous section, we suppose that an initial identification experiment has led to an initial uncertainty region \mathcal{D} for the unknown true system $G_0(z)$. The uncertainty regions delivered by prediction error identification are generally determined by bounding the so-called variance and bias errors. The variance error is due to the unavoidable presence of measurement and process noise and the bias error is present in the case where the chosen model structure is not rich enough to describe the true system [16].

Let us first consider the case where the only source of uncertainty is the noise: we therefore suppose that the true transfer function $G_0(z)$ can be parametrized by an unknown parameter vector $\theta_0 \in \mathbb{R}^k$ in a given model structure $G(z, \theta)$ i.e., $G_0(z) = G(z, \theta_0)$. In this

case, prediction error identification allows to determine an estimate $\hat{\theta}$ of θ_0 as well as an ellipsoid centered in $\hat{\theta}$ that contains the unknown θ_0 at any user-chosen probability level [16]. Let us, e.g., denote this ellipsoid $U = \{\theta \in \mathbb{R}^k \mid (\theta - \hat{\theta})^T P^{-1} (\theta - \hat{\theta}) \leq 1\}$ for some matrix $P > 0$. Since robust analysis is generally formulated for uncertain parameters lying in a ball centered at zero, we observe that U can also be rewritten as $U = \{\theta \in \mathbb{R}^k \mid \theta = \hat{\theta} + V\delta, \delta \in \mathcal{B}_k\}$ with $P = VV^T$ and $\delta \in \mathbb{R}^k$ an uncertain vector constrained to lie in the ball \mathcal{B}_k (see the notations at the end of Section 1). Knowing that the model structures used in prediction error identification are generally rational in θ i.e., $G(z, \theta) = (Z_N(z)\theta)/(1 + Z_D(z)\theta)$ with $Z_N(z)$ and $Z_D(z)$ row vectors containing only zeros and delays [5,7], the parametric uncertainty region \mathcal{D}^{par} for $G_0(z)$ has then the following form:

$$\mathcal{D}^{par} = \{G(z, \theta) = \frac{Z_N(z)\theta}{1 + Z_D(z)\theta} \mid \theta = \hat{\theta} + V\delta, \delta \in \mathcal{B}_k\}. \quad (12)$$

The uncertainty region \mathcal{D}^{par} in (12) thus contains transfer functions $\tilde{G}(z, \delta) \triangleq G(z, \hat{\theta} + V\delta)$ with $\delta \in \mathcal{B}_k$.

As mentioned above, in order to derive (12), prediction error identification has to be performed in a full-order model structure. Even though efficient techniques exist to determine such a full-order model structure (see [16, Chapter 10]), uncertainty regions can also be built in the case where the (stable) model $\hat{G}(z)$ of $G_0(z)$ is identified in a model structure whose order is too low to describe $G_0(z)$ [12,4,13,20]. Using these methods, given a user-chosen probability level, it can be derived that, at each frequency ω , $\Delta G(e^{j\omega T_s}) = G_0(e^{j\omega T_s}) - \hat{G}(e^{j\omega T_s})$ has the following property:

$$\begin{pmatrix} Re(\Delta G(e^{j\omega T_s})) \\ Im(\Delta G(e^{j\omega T_s})) \end{pmatrix} \in U(\omega),$$

where $U(\omega) = \{\xi \in \mathbb{R}^2 \mid \xi^T P(\omega)^{-1} \xi \leq 1\}$ is an ellipse in the Nyquist plane defined by a matrix $P(\omega) > 0$ (the ellipses $U(\omega)$ are different at each frequency i.e., the matrices $P(\omega)$ are different at each frequency). Observe that $U(\omega)$ is also equal to $U(\omega) = \{\xi \in \mathbb{R}^2 \mid \xi = V(\omega)\delta(\omega), \delta(\omega) \in \mathcal{B}_2\}$ with $P(\omega) = V(\omega)V(\omega)^T$ and with $\delta(\omega) \in \mathbb{R}^2$ the (normalized) vector describing the uncertainty at frequency ω and which is constrained to lie in the ball \mathcal{B}_2 . Consequently, the uncertainty region \mathcal{D}^{dyn} for $G_0(z)$ has the following form:

$$\begin{aligned} \mathcal{D}^{dyn} &= \{G(z) \mid G(z) \text{ is stable and } \dots \\ &\dots G(e^{j\omega T_s}) = \hat{G}(e^{j\omega T_s}) + v_P^T(\omega)\delta(\omega), \delta(\omega) \in \mathcal{B}_2\} \end{aligned} \quad (13)$$

with $v_P^T(\omega) \triangleq (1 \ j)V(\omega)$ ($j = \sqrt{-1}$).

Remark. As shown in [3,16], modulo a first-order Taylor approximation, the parametric uncertainty region

\mathcal{D}^{par} (see (12)) can be projected into a dynamic uncertainty region \mathcal{D}^{dyn} of the form (13). The obtained uncertainty set \mathcal{D}^{dyn} will therefore also contain systems with higher order than $G(z, \theta)$.

Remark. After the initial experiment, it is thus not guaranteed that $G_0(z)$ lies in the uncertainty region delivered by system identification. This indeed only holds modulo a certain probability level (say 99 %). Consequently, we can only verify the output amplitude constraint modulo this user-chosen probability level. Even though this probability level could be seen as a drawback, we in fact deem it an advantage. Indeed, in the robust control literature, the uncertainty region is just posed without mentioning how the assumption $G_0 \in \mathcal{D}$ can be verified in practice.

Remark. The fact that the true system $G_0(z)$ is a stable transfer function justifies the restriction to stable systems in the definition (13) of \mathcal{D}^{dyn} . This restriction in turn ensures that $y(t, G)$ with the expression (4) is indeed the steady-state output of G under (1). In order to guarantee the same property for \mathcal{D}^{par} , it is necessary to verify that all systems $G(z, \theta) \in \mathcal{D}^{par}$ are stable (using, e.g., the tools in [5]). In the sequel, we will assume that this stability condition is indeed verified.

Now that we have defined the uncertainty regions we will consider in this paper, we can particularize the expression (10) of y_{wc} for \mathcal{D}^{par} and \mathcal{D}^{dyn} . For the uncertainty region \mathcal{D}^{par} in (12), (10) is equivalent to:

$$y_{wc}^{par} = \max_{\tau \in \mathcal{T}} \max_{\delta \in \mathcal{B}_k} |Re(x_y^{par}(\tau, \delta))| \quad (14)$$

$$x_y^{par}(\tau, \delta) = \mathcal{A}^T \text{diag}(\tilde{G}(e^{j\omega_1 T_s}, \delta), \dots, \tilde{G}(e^{j\omega_L T_s}, \delta)) \tilde{U}(\tau) \quad (15)$$

with $\tilde{G}(z, \delta) \triangleq G(z, \hat{\theta} + V\delta)$. Conversely, for the uncertainty region \mathcal{D}^{dyn} in (13), we rewrite (10) as

$$y_{wc}^{dyn} = \max_{\tau \in \mathcal{T}} \max_{\delta(\omega_i) \in \mathcal{B}_2(i=1, \dots, L)} |Re(x_y^{dyn}(\tau, \delta(\omega_1), \dots, \delta(\omega_L)))| \quad (16)$$

$$\begin{aligned} x_y^{dyn}(\tau, \delta(\omega_1), \dots, \delta(\omega_L)) &= \dots \\ &= \mathcal{A}^T \text{diag}(G(\delta(\omega_1)), \dots, G(\delta(\omega_L))) \tilde{U}(\tau) \\ &\text{with } G(\delta(\omega_i)) \triangleq \hat{G}(e^{j\omega_i T_s}) + v_P^T(\omega_i) \delta(\omega_i) \quad i = 1, \dots, L \end{aligned} \quad (17)$$

It is important to note that the dependence of x_y^{par} (resp. x_y^{dyn}) on a system G in the uncertainty region \mathcal{D}^{par} (resp. \mathcal{D}^{dyn}) is restricted to the frequency response of this system at the frequencies ω_i ($i = 1, \dots, L$) present in the multisine (1). For \mathcal{D}^{par} , these L frequency response values can all be described by one unique uncertain vector $\delta \in \mathcal{B}_k$ while, for \mathcal{D}^{dyn} , these L frequency response values are described by L (independent) uncertain vectors $\delta(\omega_i) \in \mathcal{B}_2$ ($i = 1, \dots, L$).

Let us also note that (16) is equal to (10) for $\mathcal{D} = \mathcal{D}^{dyn}$ if, for any $G(\delta(\omega_i))$ with $\delta(\omega_i) \in \mathcal{B}_2$ and $i = 1, \dots, L$, there exists a stable $G(z) \in \mathcal{D}^{dyn}$ such that $G(e^{j\omega_i T_s}) = G(\delta(\omega_i))$ ($i = 1, \dots, L$). If this property does not hold, (16) is an upper bound for (10). This situation is classical for dynamic uncertainty regions such as \mathcal{D}^{dyn} and y_{wc}^{dyn} can be used to verify the output constraint in (5).

4 LFT representations for $x_u(\tau)$, x_y^{par} and x_y^{dyn}

In (9), (14) and (16), we see that the quantities we wish to evaluate have a similar form i.e., the maximization over uncertain variables of the absolute value of the real part of a complex scalar quantity x (respectively $x_u(\tau)$, $x_y^{par}(\tau, \delta)$ and $x_y^{dyn}(\tau, \delta(\omega_1), \dots, \delta(\omega_L))$). These three scalar quantities x are rational in the uncertain variables of which they are function. This property is crucial to be able to address the maximization problem in a tractable way i.e., using the tools of robustness analysis.

Since $x_u(\tau)$, $x_y^{par}(\tau, \delta)$ and $x_y^{dyn}(\tau, \delta(\omega_1), \dots, \delta(\omega_L))$ are rational in the uncertain variables of which they are function, these uncertain variables can be separated from the other parts in an LFT expression. As shown in Appendix A, we can thus determine complex matrices M_u , M_y^{par} and M_y^{dyn} such that:

$$\begin{aligned} x_u(\tau) &= (\tau I_{\alpha_L}) \star M_u \\ x_y^{par}(\tau, \delta) &= (\text{bdiag}(\tau I_{\alpha_L}, I_L \otimes \delta)) \star M_y^{par} \\ x_y^{dyn}(\tau, \delta(\omega_1), \dots, \delta(\omega_L)) &= \dots \\ &= (\text{bdiag}(\tau I_{\alpha_L}, \text{diag}(\delta(\omega_1), \dots, \delta(\omega_L)))) \star M_y^{dyn} \end{aligned} \quad (18)$$

with α_L as in (2) and where \star is defined at the end of Section 1.

We have already mentioned the similarity between the quantities u_{wc} , y_{wc}^{par} and y_{wc}^{dyn} that we wish to evaluate. Let us formalize this in the following proposition whose proof is straightforward.

Proposition 1 Consider (18) and the following worst-case quantity

$$x_{wc} = \max_{\Delta_i \in \Delta_i(i=0, \dots, r)} |Re(x(\Delta_0, \Delta_1, \dots, \Delta_r))| \quad (19)$$

where $x(\Delta_0, \Delta_1, \dots, \Delta_r) = (\text{bdiag}(\Delta_0, \Delta_1, \dots, \Delta_r)) \star M$ with M a known matrix and Δ_i ($i = 0, \dots, r$) known uncertainty sets. Then, u_{wc} defined in (9) is a particular case of (19) with $x = x_u(\tau)$, $M = M_u$, $r = 0$ and $\Delta_0 = \{\Delta_0 = \tau I_{\alpha_L} \mid \tau \in \mathcal{T}\}$. The quantity y_{wc}^{par} in (14) is also a particular case of (19) with $x = x_y^{par}(\tau, \delta)$, $M = M_y^{par}$, $r = 1$, $\Delta_1 = \{\Delta_1 = I_L \otimes \delta \mid \delta \in \mathcal{B}_k\}$ and the same Δ_0 as for u_{wc} . Finally, y_{wc}^{dyn} in (16) is also a particular case of (19) with $x = x_y^{dyn}(\tau, \delta(\omega_1), \dots, \delta(\omega_L))$, $M = M_y^{dyn}$, $r = L$, $\Delta_i = \{\Delta_i = \delta(\omega_i) \mid \delta(\omega_i) \in \mathcal{B}_2\}$ ($i = 1, \dots, L$) and the same Δ_0 as for u_{wc} and y_{wc}^{par} . ■

5 Computation of an upper bound for x_{wc}

5.1 Unifying result

Proposition 1 shows that the computation of y_{wc} (see (10)) can be formulated as (19) for \mathcal{D}^{par} and \mathcal{D}^{dyn} . Note that this is also the case for many other uncertainty sets such as the additive or multiplicative uncertainty sets which are classically used in the robustness analysis literature [22]. In this section, we will present a methodology to evaluate x_{wc} for an arbitrary complex scalar quantity $x(\Delta_0, \Delta_1, \dots, \Delta_r) = (bdiag(\Delta_0, \Delta_1, \dots, \Delta_r)) \star M$ (i.e., for an arbitrary matrix M and for arbitrary uncertainty sets Δ_i ($i = 0, \dots, r$)). Consequently, the results of this paper are not restricted to the case of the uncertainty sets delivered by prediction error identification.

As such, the optimization problem in (19) is NP-hard in almost all cases [22]. Robustness analysis however allows to formulate convex (and thus tractable) optimization problems which yield an upper bound x_{wc}^{ub} for x_{wc} . As shown in the robustness analysis literature, the obtained upper bounds are generally tight [22].

Let us first introduce the internal vectors $p = (p_0^T, \dots, p_r^T)^T$ and $q = (q_0^T, \dots, q_r^T)^T$ of the LFT $x(\Delta_0, \Delta_1, \dots, \Delta_r) = (bdiag(\Delta_0, \Delta_1, \dots, \Delta_r)) \star M$ i.e., $p = bdiag(\Delta_0, \Delta_1, \dots, \Delta_r)q$ (see the end of Section 1). We then have:

$$\begin{aligned} p_i &= \Delta_i q_i \quad (i = 0, \dots, r) \\ q_i &= M_i \begin{pmatrix} p \\ 1 \end{pmatrix} \quad (i = 0, \dots, r) \\ x(\Delta_0, \Delta_1, \dots, \Delta_r) &= M_x \begin{pmatrix} p \\ 1 \end{pmatrix}, \end{aligned} \quad (20)$$

with $M = (M_0^T, M_1^T, \dots, M_r^T, M_x^T)^T$.

Like in classical robustness analysis, we associate with each set Δ_i ($i = 0, \dots, r$) a so-called set of multipliers Π_i ($i = 0, \dots, r$). In a nutshell, the set of multipliers Π_i is an explicit and affine parametrization of the quadratic constraints satisfied by $(p_i^T, q_i^T)^T$ when $p_i = \Delta_i q_i$ with $\Delta_i \in \Delta_i$ [21,11,19].

Definition 1 Consider an uncertain variable Δ_i constrained to lie in the set Δ_i . We define the set of multipliers Π_i as a set of affinely parametrized Hermitian matrices Π_i that all have the following property:

$$\begin{pmatrix} \Delta_i \\ I \end{pmatrix}^* \Pi_i \begin{pmatrix} \Delta_i \\ I \end{pmatrix} \geq 0 \quad \forall \Delta_i \in \Delta_i. \quad (21)$$

In other words, $\Pi_i \in \Pi_i \implies (21)$.

Using the sets of multipliers Π_i ($i = 0, \dots, r$), we can now develop the following LMI optimization problem whose solution is an upper bound x_{wc}^{ub} for x_{wc} .

Proposition 2 Consider a complex scalar quantity $x(\Delta_0, \dots, \Delta_r)$ depending as in (20) on $r + 1$ uncertain variables $\Delta_i \in \Delta_i$ ($i = 0, \dots, r$) and consider the sets of multipliers Π_i ($i = 0, \dots, r$) for each uncertainty set Δ_i ($i = 0, \dots, r$) (see Definition 1). Then, an upper bound x_{wc}^{ub} for x_{wc} (see (19)) is the solution γ_{opt} of the following LMI optimization problem having as decision variables a real scalar $\gamma \geq 0$ and two matrices Π_i^1, Π_i^2 within each of the sets of multipliers Π_i ($i = 0, \dots, r$):

$$\min \gamma \text{ s.t.} \quad (22)$$

$$\mathcal{G}_x^* \begin{pmatrix} -\gamma & 0.5 \\ 0.5 & 0 \end{pmatrix} \mathcal{G}_x + \sum_{i=0}^r \mathcal{G}_i^* \Pi_i^1 \mathcal{G}_i \leq 0 \quad (23)$$

$$0 \leq \mathcal{G}_x^* \begin{pmatrix} \gamma & 0.5 \\ 0.5 & 0 \end{pmatrix} \mathcal{G}_x - \sum_{i=0}^r \mathcal{G}_i^* \Pi_i^2 \mathcal{G}_i \quad (24)$$

with $\mathcal{G}_x = (Z_x^T M_x^T)^T$ and $\mathcal{G}_i = (Z_i^T M_i^T)^T$ ($i = 0, \dots, r$) (Z_x and Z_i ($i = 0, \dots, r$) are selection matrices such that $Z_x(p^T 1)^T = 1$ and $Z_i(p^T 1)^T = p_i$ ($i = 0, \dots, r$)).

Proof. The result follows from the fact that (23) and (24) imply

$$-\gamma \leq \text{Re}(x(\Delta_0, \dots, \Delta_r)) \leq \gamma \quad \forall \Delta_i \in \Delta_i \quad (i = 0, \dots, r) \quad (25)$$

Let us thus prove this result. For this purpose, let us consider one value of $\Delta = bdiag(\Delta_0, \Delta_1, \dots, \Delta_r)$ in the LFT (20) and let us consider the corresponding internal vectors $p = (p_0^T, \dots, p_r^T)^T$ and $q = (q_0^T, \dots, q_r^T)^T$. Let us then pre- and post-multiply with $(p^*, 1)$ and $(p^T, 1)^T$ the LMI constraints (23) and (24). Using (20), this yields

$$\text{Re}(x(\Delta_0, \dots, \Delta_r)) + \sum_{i=0}^r g_i^* \Pi_i^1 g_i \leq \gamma \quad (26)$$

$$-\gamma \leq \text{Re}(x(\Delta_0, \dots, \Delta_r)) - \sum_{i=0}^r g_i^* \Pi_i^2 g_i \quad (27)$$

with $g_i = (p_i^T, q_i^T)^T$ ($i = 0, \dots, r$). The above reasoning can be done for any value of $\Delta = bdiag(\Delta_0, \Delta_1, \dots, \Delta_r)$ with $\Delta_i \in \Delta_i$ ($i = 0, \dots, r$). In other words, for the multipliers Π_i^1, Π_i^2 ($i = 0, \dots, r$) found by the optimization problem, (26) and (27) hold true for all $\Delta_i \in \Delta_i$ ($i = 0, \dots, r$). Observe also that, because of (20), $g_i = (\Delta_i^T \ I)^T q_i$. Consequently, due to Definition 1, we have that $\sum_{i=0}^r g_i^* \Pi_i^1 g_i$ in (26) is positive for all $\Delta_i \in \Delta_i$ ($i = 0, \dots, r$). Similarly, $-\sum_{i=0}^r g_i^* \Pi_i^2 g_i$ in (27) is negative for all $\Delta_i \in \Delta_i$ ($i = 0, \dots, r$). We have thus proven that (23) and (24) imply (25). ■

It is clear that the more general the parametrization of the sets of multipliers Π_i ($i = 0, \dots, r$), the tighter the upper bound of x_{wc} delivered by the LMI optimization problem (22)-(24) [21,11,19]. In the next section, we will make use of the fact that, for all the quantities we wish to evaluate in this paper, the uncertainty set Δ_0 is given

by $\mathbf{\Delta}_0 = \{\Delta_0 = \tau I_{\alpha L} \mid \tau \in \mathcal{T}\}$ i.e., a simple uncertainty set based on a scalar uncertain variable $\tau \in \mathcal{T}$. The fact that Δ_0 has a simple structure allows to use Δ_0 -dependent multipliers Π_i for all other uncertain variables $\Delta_i \in \mathbf{\Delta}_i$ ($i = 1, \dots, r$). Even though this will lead to a slightly more complex LMI optimization problem, the upper bound x_{wc}^{ub} for x_{wc} obtained in this way will generally be tighter (see, e.g., [2]). In order to justify this approach, let us consider, for any $\Delta_0 \in \mathbf{\Delta}_0$, the quantity $x_{wc}(\Delta_0) = \max_{\Delta_i \in \mathbf{\Delta}_i (i=1, \dots, r)} |Re(x(\Delta_0, \Delta_1, \dots, \Delta_r))|$ and let us note that $x_{wc} = \max_{\Delta_0 \in \mathbf{\Delta}_0} x_{wc}(\Delta_0)$. If we evaluate the upper bound of $x_{wc}(\Delta_0)$ via a multiplier approach similar to the one in Proposition 2, the multipliers Π_i^1 and Π_i^2 ($i = 1, \dots, r$) can be different for each value of Δ_0 and this thus advocates to consider Δ_0 -dependent multipliers Π_i ($i = 1, \dots, r$) to compute x_{wc}^{ub} .

5.2 Improvement for the case $\Delta_0 = \tau I_\alpha$

Let us thus particularize the LFT (20) to $p_0 = \tau I_\alpha q_0$ for some integer α and let us consider the following factorization of the multipliers Π_i ($i = 1, \dots, r$) given in Definition 1.

Definition 2 Consider the variable τ lying in the set \mathcal{T} (see (11)) and the set $\mathbf{\Pi}_i$ of multipliers for the uncertain variable $\Delta_i \in \mathbf{\Delta}_i$ (see Definition 1). The τ -dependent factorization corresponding to $\mathbf{\Pi}_i$ is defined via a matrix $\Psi_i(\tau)$ rational in τ and a set \mathbf{P}_i of affinely parametrized (τ -independent) Hermitian matrices \mathcal{P}_i . These elements are determined in such a way that, for each $\tau \in \mathcal{T}$ and for each $\mathcal{P}_i \in \mathbf{P}_i$, $\Psi_i^*(\tau)\mathcal{P}_i\Psi_i(\tau)$ are elements of $\mathbf{\Pi}_i$.

Using the matrices $\Psi_i(\tau)$ introduced in Definition 2, the LFT (20) and the quantity \mathcal{G}_i defined below (24), we pose:

$$g_{\Psi,i} = \Psi_i(\tau)\mathcal{G}_i \begin{pmatrix} p \\ 1 \end{pmatrix} \quad (i = 1, \dots, r). \quad (28)$$

Since all $\Psi_i(\tau)$ ($i = 1, \dots, r$) are rational in τ , $g_\Psi = (g_{\Psi,1}^T, \dots, g_{\Psi,r}^T)^T$ can be expressed as:

$$g_\Psi = \begin{pmatrix} (\tau I_\beta) \star \underbrace{\begin{pmatrix} \mathcal{M}_{11} & \mathcal{M}_{12} \\ \mathcal{M}_{21} & \mathcal{M}_{22} \end{pmatrix}}_{=\mathcal{M}} \end{pmatrix} \begin{pmatrix} p \\ 1 \end{pmatrix} \quad (29)$$

for some integer β and for some matrix \mathcal{M} . For further use, let us introduce the internal signals p_Ψ and q_Ψ of the LFT (29):

$$\begin{aligned} p_\Psi &= \tau I_\beta q_\Psi \\ q_\Psi &= \mathcal{M}_{11} p_\Psi + \mathcal{M}_{12} \begin{pmatrix} p \\ 1 \end{pmatrix} \\ g_{\Psi,i} &= \mathcal{M}_{21,i} p_\Psi + \mathcal{M}_{22,i} \begin{pmatrix} p \\ 1 \end{pmatrix} \quad (i = 1, \dots, r), \end{aligned} \quad (30)$$

with $(\mathcal{M}_{21,i} \mathcal{M}_{22,i}) = R_i(\mathcal{M}_{21} \mathcal{M}_{22})$ where R_i is a selection matrix such that $g_{\Psi,i} = R_i g_\Psi$ ($i = 1, \dots, r$). We have now all the ingredients to obtain an alternative LMI optimization problem yielding an upper bound for x_{wc} . If the factorization in Definition 2 is chosen with care (the more general, the better), we can expect that this upper bound will be tighter than the one given in Proposition 2 since it is derived with τ -dependent multipliers [2].

Proposition 3 Consider the framework of Proposition 2 with $\mathbf{\Delta}_0 = \{\Delta_0 = \tau I_\alpha \mid \tau \in \mathcal{T}\}$. Consider also the factorization of the multipliers Π_i ($i = 1, \dots, r$) (see Definition 2) and the notations (28)-(30). Consider finally the set of multiplier $\tilde{\mathbf{\Pi}}_0$ corresponding to $\mathbf{\Delta}_0 = \{\tilde{\Delta}_0 = \tau I_\rho \mid \tau \in \mathcal{T}\}$ with $\rho = \alpha + \beta$ (see Definition 1). Then, an upper bound for x_{wc} is the solution γ_{opt} of the following LMI optimization problem having as decision variables a real scalar $\gamma \geq 0$, two matrices $\tilde{\Pi}_0^1$ and $\tilde{\Pi}_0^2$ in $\tilde{\mathbf{\Pi}}_0$ and two matrices $\mathcal{P}_i^1, \mathcal{P}_i^2$ within each set \mathbf{P}_i ($i = 1, \dots, r$) (see Definition 2):

$$\min \gamma \text{ s.t.} \quad (31)$$

$$\mathcal{V}_1^* \begin{pmatrix} -\gamma & 0.5 \\ 0.5 & 0 \end{pmatrix} \mathcal{V}_1 + \mathcal{V}_2^* \tilde{\Pi}_0^1 \mathcal{V}_2 + \sum_{i=1}^r \mathcal{R}_i^* \mathcal{P}_i^1 \mathcal{R}_i \leq 0 \quad (32)$$

$$0 \leq \mathcal{V}_1^* \begin{pmatrix} \gamma & 0.5 \\ 0.5 & 0 \end{pmatrix} \mathcal{V}_1 - \mathcal{V}_2^* \tilde{\Pi}_0^2 \mathcal{V}_2 - \sum_{i=1}^r \mathcal{R}_i^* \mathcal{P}_i^2 \mathcal{R}_i, \quad (33)$$

where $\mathcal{V}_1 = (0 \ \mathcal{G}_x)$, $\mathcal{R}_i = (\mathcal{M}_{21,i} \ \mathcal{M}_{22,i})$ and

$$\mathcal{V}_2 = \begin{pmatrix} \text{bdiag}(I_\beta, Z_0) \\ \begin{pmatrix} \mathcal{M}_{11} & \mathcal{M}_{12} \\ 0 & M_0 \end{pmatrix} \end{pmatrix}$$

with \mathcal{G}_x and Z_0 defined below (24) and with M_0 defined in (20).

Proof. The result follows here also from the fact that (32) and (33) imply (25). Let us thus prove this result. For this purpose, let us consider one value of $\Delta = \text{bdiag}(\Delta_0 = \tau I_\alpha, \Delta_1, \dots, \Delta_r)$ in the LFT (20) and let us consider the same τ in the LFT (30). With the corresponding internal vectors $p = (p_0^T, \dots, p_r^T)^T$ and $q = (q_0^T, \dots, q_r^T)^T$ (see (20)) and the corresponding vectors p_Ψ and q_Ψ (see (30)), let us pre- and post-multiply with $(p_\Psi^*, p^*, 1)$ and $(p_\Psi^T, p^T, 1)^T$ the LMI constraints (32) and (33). Using (20), (28) and (30), this yields

$$Re(x(\tau, \Delta_1, \dots, \Delta_n)) + g_\tau^* \tilde{\Pi}_0^1 g_\tau + \sum_{i=1}^r g_i^* \Psi_i^*(\tau) \mathcal{P}_i^1 \Psi_i(\tau) g_i \leq \gamma \quad (34)$$

$$-\gamma \leq Re(x(\tau, \Delta_1, \dots, \Delta_n)) - g_\tau^* \tilde{\Pi}_0^2 g_\tau - \sum_{i=1}^r g_i^* \Psi_i^*(\tau) \mathcal{P}_i^2 \Psi_i(\tau) g_i \quad (35)$$

with $g_\tau = (p_\psi^T, p_0^T, q_\psi^T, q_0^T)^T$ and $g_i = (p_i^T \ q_i^T)^T = \mathcal{G}_i(p^T \ 1)^T$ ($i = 1, \dots, r$). The above reasoning can be done for any value of $\tau \in \mathcal{T}$ and of $\Delta_i \in \mathbf{\Delta}_i$ ($i = 1, \dots, r$). In other words, for the multipliers $\tilde{\Pi}_0^1, \tilde{\Pi}_0^2, \mathcal{P}_i^1$ and \mathcal{P}_i^2 ($i = 1, \dots, r$) found by the optimization problem, (34) and (35) hold true for all $\tau \in \mathcal{T}$ and for all $\Delta_i \in \mathbf{\Delta}_i$ ($i = 1, \dots, r$). Observe also that, because of (20) and (30), $g_i = (\Delta_i^T \ I)^T q_i$ and $g_\tau = (\tau I_\rho \ I_\rho)^T (q_\psi^T, q_0^T)^T$. Consequently, due to Definitions 1 and 2, we have that $g_\tau^* \tilde{\Pi}_0^1 g_\tau + \sum_{i=1}^r g_i^* \Psi_i^*(\tau) \mathcal{P}_i^1 \Psi_i(\tau) g_i$ in (34) is positive for all $\tau \in \mathcal{T}$ and for all $\Delta_i \in \mathbf{\Delta}_i$ ($i = 1, \dots, r$). Similarly, $-g_\tau^* \tilde{\Pi}_0^2 g_\tau - \sum_{i=1}^r g_i^* \Psi_i^*(\tau) \mathcal{P}_i^2 \Psi_i(\tau) g_i$ in (35) is negative for all $\tau \in \mathcal{T}$ and for all $\Delta_i \in \mathbf{\Delta}_i$ ($i = 1, \dots, r$). We have thus proven that (32) and (33) imply (25). ■

6 Upper bounds for u_{wc} , y_{wc}^{par} and y_{wc}^{dyn}

We will now use the results of the previous section to derive tight upper bounds for u_{wc} , y_{wc}^{par} and y_{wc}^{dyn} . For this purpose, we however still need to present the sets of multipliers corresponding to the type of uncertainties encountered in (18). Let us start with the set of multipliers corresponding to $\mathbf{\Delta}_0 = \{\Delta_0 = \tau I_\alpha \mid \tau \in \mathcal{T}\}$ for an arbitrary α (in Proposition 1, $\alpha = \alpha_L$).

Proposition 4 Consider $\mathbf{\Delta}_0 = \{\Delta_0 = \tau I_\alpha \mid \tau \in \mathcal{T}\}$ with the set \mathcal{T} defined in (11) and an arbitrary scalar α . Then,

$$\begin{pmatrix} \Delta_0 \\ I \end{pmatrix}^* \Xi_\alpha \begin{pmatrix} \Delta_0 \\ I \end{pmatrix} \leq 0 \quad \forall \Delta_0 \in \mathbf{\Delta}_0 \quad (36)$$

when $\Xi_\alpha = bdiag(S, -S)$ with S any Hermitian matrix of dimension $\alpha \times \alpha$. The set of matrices Ξ_α having this structure will be denoted $\mathbf{\Xi}_\alpha$ in the sequel.

Proof. For any $\Xi_\alpha = bdiag(S, -S)$, we have that the quadratic expression in (36) is equal to $(\tau^* \tau - 1)S$ and this quantity is indeed larger or equal to zero for all $\tau \in \mathcal{T}$ (since it is in fact identically equal to zero for all $\tau \in \mathcal{T}$). ■

Let us also present the set of multipliers corresponding to $\mathbf{\Delta}_i = \{\Delta_i = I_m \otimes \delta \mid \delta \in \mathcal{B}_n\}$ for arbitrary integers m and n (in Proposition 1, $m = L$ and $n = k$ for the case of y_{wc}^{par} and $m = 1$ and $n = 2$ for the case of y_{wc}^{dyn}). A very general parametrization of the set of multipliers corresponding to this uncertainty has been developed in our previous contribution [1].

Proposition 5 ([1]) Consider the set $\mathcal{B}_n = \{\delta \in \mathbb{R}^n \mid \delta^T \delta \leq 1\}$ and an arbitrary integer m . Then,

$$\begin{pmatrix} I_m \otimes \delta \\ I_m \end{pmatrix}^T \Sigma_{m,n} \begin{pmatrix} I_m \otimes \delta \\ I_m \end{pmatrix} \geq 0 \quad \forall \delta \in \mathcal{B}_n \quad (37)$$

when $\Sigma_{m,n}$ has the following structure

$$\Sigma_{m,n} = \left(\begin{array}{c|c} -Q \otimes I_n + \tilde{B} + j \tilde{D} & \tilde{P}^T - j \tilde{Z}^T \\ \hline \tilde{P} + j \tilde{Z} & Q \end{array} \right) \quad (38)$$

where Q is any positive semi-definite Hermitian matrix of dimension $m \times m$ and $\tilde{B}, \tilde{D}, \tilde{P}, \tilde{Z}$ real matrices having the structure given in Appendix B. The set of matrices $\Sigma_{m,n}$ having the structure (38) will be denoted $\mathbf{\Sigma}_{m,n}$ in the sequel. ■

In order to be able to use Proposition 3 to improve the upper bound for y_{wc}^{par} and y_{wc}^{dyn} , we develop in the next proposition a τ -dependent factorization of the set of multipliers introduced in Proposition 5. This factorization is more general than the one given in [6]. In this proposition, we will use the following vector $\mathcal{N}(\tau) = (1, \tau, \tau^2, \dots, \tau^b)^T$ where b is an arbitrary integer and which can be written as the LFT $\mathcal{N}(\tau) = (\tau I_b) \star \tilde{\mathcal{N}}$ with

$$\underbrace{\begin{pmatrix} \tilde{\mathcal{N}}_{11} & \tilde{\mathcal{N}}_{12} \\ \tilde{\mathcal{N}}_{21} & \tilde{\mathcal{N}}_{22} \end{pmatrix}}_{=\tilde{\mathcal{N}}} = \left(\begin{array}{c|c} \begin{pmatrix} 0 & 0 \\ I_{b-1} & 0 \end{pmatrix} & (1, 0, \dots, 0)^T \\ \hline (0, I_b)^T & (1, 0, \dots, 0)^T \end{array} \right) \quad (39)$$

Proposition 6 Consider the set of multipliers $\mathbf{\Sigma}_{m,n}$ linked to $I_m \otimes \delta$ with $\delta \in \mathcal{B}_n$ (see Proposition 5). Consider also the variable τ that varies in the set \mathcal{T} (see (11)). Using τ and some user-chosen integer $b \geq 1$, define the vector $\mathcal{N}(\tau) = (1, \tau, \tau^2, \dots, \tau^b)^T$ and the matrix $\Psi_{\Sigma_{m,n}}(\tau)$:

$$\Psi_{\Sigma_{m,n}}(\tau) = \begin{pmatrix} \mathcal{N}(\tau) \otimes I_{nm} & 0 \\ 0 & \mathcal{N}(\tau) \otimes I_m \\ I_{nm} & 0 \\ 0 & I_m \end{pmatrix}. \quad (40)$$

Then, for each $\tau \in \mathcal{T}$, the τ -dependent matrices $\Psi_{\Sigma_{m,n}}^*(\tau) \mathcal{P}_{\Sigma_{m,n}} \Psi_{\Sigma_{m,n}}(\tau)$ with $\mathcal{P}_{\Sigma_{m,n}} \in \mathbf{P}_{\Sigma_{m,n}}$ are all elements $\Sigma_{m,n}$ of $\mathbf{\Sigma}_{m,n}$. The set $\mathbf{P}_{\Sigma_{m,n}}$ contains all matrices $\mathcal{P}_{\Sigma_{m,n}}$ having the following structure:

$$\mathcal{P}_{\Sigma_{m,n}} = \left[\begin{array}{cc} [-\Lambda \otimes I_n & 0] \\ 0 & \Lambda \end{array} \right] \mathcal{P}_{21}^T \quad \text{with } \Lambda = \begin{pmatrix} Q_0 & \dots & Q_b \\ \vdots & 0 & 0 \\ Q_b^* & 0 & 0 \end{pmatrix}$$

$$\mathcal{P}_{21} = \left(\begin{array}{c|c} (\tilde{B}_0, \dots, \tilde{B}_b) + (0, \tilde{D}_1, \dots, \tilde{D}_b) & \begin{pmatrix} \tilde{P}_0 \\ \dots \\ \tilde{P}_b \end{pmatrix}^T - \begin{pmatrix} 0 \\ \tilde{Z}_1 \\ \tilde{Z}_b \end{pmatrix}^T \\ \hline (0, \tilde{Z}_1, \dots, \tilde{Z}_b) + (\tilde{P}_0, \dots, \tilde{P}_b) & 0 \end{array} \right)$$

$$\mathcal{P}_{22} = \begin{pmatrix} j\tilde{D}_0 & -j\tilde{Z}_0^T \\ j\tilde{Z}_0 & 0 \end{pmatrix}.$$

The real matrices \tilde{B}_i , \tilde{D}_i , \tilde{P}_i and \tilde{Z}_i ($i = 0, \dots, b$) of the parametrization of $\mathcal{P}_{\Sigma_{m,n}}$ can take any values provided that they have, respectively, the same structure as the real matrices \tilde{B} , \tilde{D} , \tilde{P} and \tilde{Z} in (38). Finally, the elements of the matrix Λ are constrained as follows: $Q_i \in \mathbb{C}^{m \times m}$ ($i = 1 \dots b$), $Q_0 = Q_0^* \in \mathbb{C}^{m \times m}$ and there must exist a matrix $\Xi_{bm} \in \Xi_{bm}$ (see Proposition 4) such that the following LMI is satisfied:

$$0 \leq - \begin{pmatrix} I & 0 \\ \tilde{N}_{m,11} & \tilde{N}_{m,12} \end{pmatrix}^* \Xi_{bm} \begin{pmatrix} I & 0 \\ \tilde{N}_{m,11} & \tilde{N}_{m,12} \end{pmatrix} + \dots \\ \dots + \begin{pmatrix} \tilde{N}_{m,21} & \tilde{N}_{m,22} \end{pmatrix}^* \Lambda \begin{pmatrix} \tilde{N}_{m,21} & \tilde{N}_{m,22} \end{pmatrix} \quad (41)$$

where $\tilde{N}_{m,11} = \tilde{N}_{11} \otimes I_m$, $\tilde{N}_{m,12} = \tilde{N}_{12} \otimes I_m$, $\tilde{N}_{m,21} = \tilde{N}_{21} \otimes I_m$ and $\tilde{N}_{m,22} = \tilde{N}_{22} \otimes I_m$ (see (39)).

Proof. See Appendix C. \blacksquare

We have now all the ingredients to derive upper bounds for u_{wc} , y_{wc}^{par} and y_{wc}^{dyn} defined, respectively, in (9), (14) and (16). Let us begin with u_{wc} . Using Proposition 1, it is clear that the upper bound for u_{wc} is the solution γ_{opt} of the LMI optimization problem (22)-(24) with $r = 0$, $\Pi_0 = \Xi_{\alpha_L}$ (see Proposition 4) and with M_x , M_0 (see (20)) obtained from the decomposition of M_u . Note that we have here in fact a stronger result.

Proposition 7 Consider the LMI optimization problem (22)-(24) with $r = 0$, $\Pi_0 = \Xi_{\alpha_L}$ (see Proposition 4) and with M_x , M_0 (see (20)) obtained from the decomposition of M_u . Then, the solution γ_{opt} of (22)-(24) is equal to u_{wc} .

Proof. see Appendix D. \blacksquare

Let us now turn to y_{wc}^{par} and y_{wc}^{dyn} . Using Propositions 1, 2 and 3, we have the following results whose proofs are straightforward:

Proposition 8 Consider the LMI optimization problem (22)-(24) with $r = 1$, $\Pi_0 = \Xi_{\alpha_L}$ (see Proposition 4), $\Pi_1 = \Sigma_{L,k}$ (see Proposition 5) and with M_x , M_0 , M_1 (see (20)) obtained from the decomposition of M_y^{par} . Then, the solution γ_{opt} of (22)-(24) is an upper bound for y_{wc}^{par} (see (14)). We can also consider the procedure in Section 5.2 to try to improve this upper bound. Since $r = 1$ and $\Pi_1 = \Sigma_{L,k}$, we have that $\Psi_1(\tau) = \Psi_{\Sigma_{L,k}}(\tau)$ (see Proposition 6) and thus (29) can be written with $\beta = bL(k+1)$ and with a matrix \mathcal{M} that can be derived from the LFT of $\mathcal{N}(\tau)$ (see (39)). A (generally tighter)

upper bound for y_{wc}^{par} can thus be obtained as the solution γ_{opt} of the LMI optimization problem (31)-(33) with $r = 1$, $\tilde{\Pi}_0 = \Xi_{\rho}$ (see Proposition 4), $\rho = \alpha_L + bL(k+1)$ and with $\mathbf{P}_1 = \mathbf{P}_{\Sigma_{L,k}}$ (see Proposition 6). \blacksquare

Proposition 9 Consider the LMI optimization problem (22)-(24) with $r = L$, $\Pi_0 = \Xi_{\alpha_L}$ (see Proposition 4), $\Pi_i = \Sigma_{1,2}$ for $i = 1, \dots, L$ (see Proposition 5) and with M_x , M_i ($i = 0, \dots, L$) obtained from the decomposition of M_y^{dyn} . Then, the solution γ_{opt} of (22)-(24) is an upper bound for y_{wc}^{dyn} (see (16)). We can also consider the procedure in Section 5.2 to try to improve this upper bound. Since $r = L$ and $\Pi_i = \Sigma_{1,2}$ for $i = 1, \dots, L$, we have that $\Psi_i(\tau) = \Psi_{\Sigma_{1,2}}(\tau)$ for $i = 1, \dots, L$ and thus (29) can be written with $\beta = 3bL$ and with a matrix \mathcal{M} that can be derived from the LFT of $\mathcal{N}(\tau)$ (see (39)). A (generally tighter) upper bound for y_{wc}^{dyn} can thus be obtained as the solution γ_{opt} of the LMI optimization problem (31)-(33) with $r = L$, $\tilde{\Pi}_0 = \Xi_{\rho}$, $\rho = \alpha_L + 3bL$ and with $\mathbf{P}_i = \mathbf{P}_{\Sigma_{1,2}}$ for $i = 1, \dots, L$. \blacksquare

Remark. The LMI constraint (41) on the parametrization of the elements of $\mathbf{P}_{\Sigma_{L,k}}$ (resp. $\mathbf{P}_{\Sigma_{1,2}}$) in Proposition 8 (resp. in Proposition 9) can be easily added as an extra LMI constraint in the LMI optimization problem (31)-(33).

Remark. We can verify the tightness of the obtained upper bound y_{wc}^{ub} for y_{wc} (i.e., either y_{wc}^{par} or y_{wc}^{dyn}) by computing a lower bound y_{wc}^{lb} for y_{wc} using a gridding of the uncertainty region \mathcal{D} (i.e., either \mathcal{D}^{par} or \mathcal{D}^{dyn}) and a gridding of the interval T_P i.e., $y_{wc}^{lb} = \max_{t \in T_{P,grid}} \max_{G(z) \in \mathcal{D}_{grid}} |y(t, G)|$ where $T_{P,grid}$ is a discrete set containing a finite number of the time instants $t \in T_P$ and where \mathcal{D}_{grid} is a discrete set which contains a finite number of the systems lying in \mathcal{D} .

Remark. Note also that, as opposed to its upper bound y_{wc}^{ub} , the lower bound y_{wc}^{lb} for y_{wc} is not sufficient to verify the output amplitude constraint in (5). This constraint can indeed be verified by checking that $y_{wc}^{ub} \leq \bar{y}_{max}$ since the latter implies $y_{wc} \leq \bar{y}_{max}$. As opposed to this, $y_{wc}^{lb} \leq \bar{y}_{max}$ does not imply $y_{wc} \leq \bar{y}_{max}$ since $y_{wc}^{lb} \leq y_{wc}$. The above reasoning of course assumes that $G_0 \in \mathcal{D}$. In the rare cases where that will not be the case (the uncertainty region \mathcal{D} only contains G_0 modulo a certain probability level), it can then happen that the largest value of $|y(t, G_0)|$ is larger than y_{wc}^{ub} . However, in these cases, the upper bound y_{wc}^{ub} remains a closer estimate of the largest value of $|y(t, G_0)|$ than y_{wc}^{lb} since $y_{wc}^{ub} > y_{wc}^{lb}$.

Remark. Besides u_{wc} , y_{wc}^{par} and y_{wc}^{dyn} , the results in Section 5 allows to compute upper bounds for other quantities. First, as already mentioned, they allow to compute upper bounds for y_{wc} (see (7)) for other types of uncertainty regions. They also allow to evaluate an upper

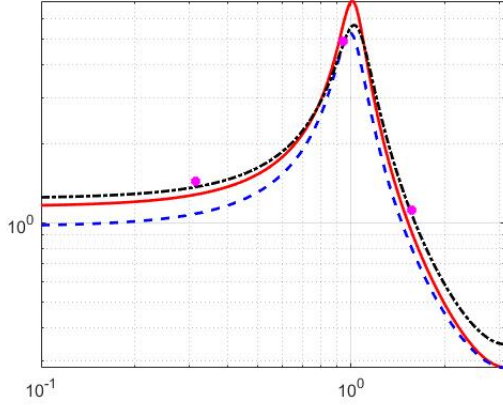


Fig. 1. Magnitude plot of $G_0(z)$ (red solid) of $G(z, \hat{\theta})$ (blue dashed) and of $G_{grid}^{par}(z)$ (black dashdot). The magenta dots indicate $|G_{grid}^{dyn}(e^{j\omega_i T_s})|$ for ω_i ($i = 1, 2, 3$).

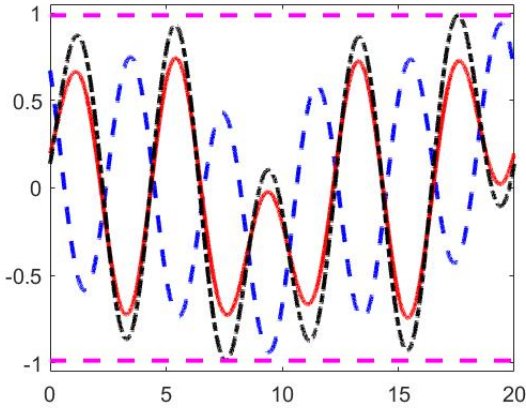


Fig. 2. One period of $u(t)$ (blue dashed), of $y(t, \hat{G})$ (red solid) and of $y(t, G_{grid}^{par})$ (black dashdot). The dashed magenta lines indicate ± 0.986550 .

bound for the worst case output amplitude *at a given time instant* t i.e., $y_{wc}(t) = \max_{G(z) \in \mathcal{D}} |y(t, G)|$. As another example, using a similar procedure as for the computation of u_{wc} , Proposition 2 also allows to compute the worst case output amplitude *for a given plant* G_{given} i.e., $y_{wc}(G_{given}) = \max_{t \in T_P} |y(t, G_{given})|$.

7 Numerical illustration

We consider here a second-order true system $G_0(z) = G(z, \theta_0) = (\theta_{0,1}z^{-1} + \theta_{0,2}z^{-2}) / (1 + \theta_{0,3}z^{-1} + \theta_{0,4}z^{-2})$ with $\theta_0 = (\theta_{0,1}, \theta_{0,2}, \theta_{0,3}, \theta_{0,4})^T = (0.8988, 0.1034, -0.9723, 0.8385)^T$. The sampling rate is $T_s = 1$ s. An initial identification experiment in a full-order model structure has delivered an identified model $G(z, \hat{\theta})$ with $\hat{\theta} = (0.8 \ 0.01 \ -0.9854 \ 0.8187)^T$ as well as an ellipsoid $U = \{\theta \mid (\theta - \hat{\theta})^T P^{-1}(\theta - \hat{\theta}) \leq 1\}$ described by the matrix P^{-1} :

$$P^{-1} = \begin{pmatrix} 33.1902 & 19.8594 & -49.0182 & 28.3717 \\ 19.8594 & 33.1902 & -98.2813 & -49.0182 \\ -49.0182 & -98.2813 & 435.6784 & 258.1596 \\ 28.3717 & -49.0182 & 258.1596 & 435.6784 \end{pmatrix}.$$

These elements define the parametric uncertainty region \mathcal{D}^{par} in (12) which here contains the true system $G_0(z)$ (i.e., $\theta_0 \in U$). In Figure 1, we represent the magnitude plot of both G_0 and $G(z, \hat{\theta})$.

We consider a multisine excitation $u(t)$ (see (1)) of fundamental frequency $\omega_0 = 0.1\pi$ rad/s (the period T_0 is thus 20 s) and containing $L = 3$ frequencies i.e., $\omega_1 = \omega_0$, $\omega_2 = 3\omega_0$ and $\omega_3 = 5\omega_0$. The complex amplitude vector \mathcal{A} in the phasor notation (3) is here chosen as $\mathcal{A} = (0.2212 + 0.0688j, -0.0120 + 0.0662j, 0.4621 + 0.5075j)^T$. This amplitude vector has been determined using the optimal experiment design procedure of [9]. Using the LMI procedure of Proposition 7 for this multisine $u(t)$, we obtain $u_{wc} = 0.9385$ which is consistent with what can be observed in Figure 2 where the maximal value of $|u(t)|$ is indeed 0.9385.

As shown in Figure 2, when applied to $\hat{G}(z) = G(z, \hat{\theta})$, this multisine $u(t)$ yields a multisine output $y(t, \hat{G})$ with a maximal amplitude of 0.7425. The maximal amplitude of $y(t, G_0)$ is equal to 0.9070. Let us now consider the worst-case amplitude y_{wc}^{par} in \mathcal{D}^{par} (see (14)). This quantity will be larger than 0.9070 since $G_0 \in \mathcal{D}^{par}$. If we use the LMI optimization problem (22)-(24) (see Proposition 8), we obtain the following upper bound for y_{wc}^{par} : $y_{wc}^{par,ub} = 1$. If we use the LMI optimization problem (31)-(33) with the τ -dependent multiplier for $b = 1$ (see Proposition 8), we obtain $y_{wc}^{par,ub} = 0.986550$. Let us analyze the tightness of these upper bounds. For this purpose, we observe (see Figure 2) that the output $y(t, G_{grid}^{par})$ corresponding to a system $G_{grid}^{par}(z) \in \mathcal{D}^{par}$ has a maximal amplitude equal to 0.986535 i.e., $y_{wc}^{par,lb} = 0.986535$. The conservatism linked to the LMI procedure (22)-(24) is thus in this example less than 1.4 % (which is small) and the one linked to the LMI procedure (31)-(33) with $b = 1$ is less than 0.001 % (which is negligible). This shows the efficiency of the proposed procedure to evaluate the worst case amplitude of the output over the systems in \mathcal{D}^{par} . It is to be noted that the system $G_{grid}^{par}(z)$ has been determined by a smart gridding procedure called Bayesian optimization [10]. This system is described by $G_{grid}^{par}(z) = G(z, \theta_{grid})$ with $\theta_{grid} = (1.007, 0.072, -0.9152, 0.7842)^T \in U$. See Figure 1 for the magnitude plot of $G_{grid}^{par}(z)$. It is important to note that this smart gridding procedure is not a valid alternative for the approach developed in this paper. The main reason for that is that it only delivers a lower bound for y_{wc}^{par} while an upper bound is necessary to verify the output amplitude constraint in (5) (see the third remark at the end of Section 6). Another reason is that this smart gridding procedure is twenty times

more time consuming than the LMI optimization problem (22)-(24) and two times more time consuming than the LMI optimization problem (31)-(33).

Let us now consider y_{wc}^{dyn} when \mathcal{D}^{dyn} is the dynamic uncertainty region (13) obtained by projecting \mathcal{D}^{par} into the Nyquist plane (see the first remark in Section 3). Since this \mathcal{D}^{dyn} will not only contain systems of the second order, but also systems of higher order, we therefore expect that $y_{wc}^{dyn} > y_{wc}^{par}$. If we use the LMI optimization problem (22)-(24) (see Proposition 9), we obtain the following upper bound for y_{wc}^{dyn} : $y_{wc}^{dyn,ub} = 1.1388$. If we use the LMI optimization problem (31)-(33) with the τ -dependent multiplier for $b = 1$ (see Proposition 9), we obtain $y_{wc}^{par,ub} = 1.1065$. Let us analyze the tightness of these upper bounds. For this purpose, we have determined, using Bayesian optimization, three points $G_{grid}^{dyn}(e^{j\omega_i T_s})$ ($i = 1, 2, 3$) such that $(Re(G_{grid}^{dyn}(e^{j\omega_i T_s})), Im(G_{grid}^{dyn}(e^{j\omega_i T_s})))^T \in U(\omega_i)$ ($i = 1, 2, 3$) where $U(\omega_i)$ is the ellipse $U(\omega)$ defining \mathcal{D}^{dyn} for the frequency ω_i in the multisine ($i = 1, 2, 3$). For these points, we determine, via (4), the multisine $y(t, G_{grid}^{dyn})$ which has a maximal amplitude of 1.106342 i.e., $y_{wc}^{dyn,lb} = 1.106342$. The conservatism linked to the LMI procedure (22)-(24) is thus in this example less than 2.9 % (which is small) and the one linked to the LMI procedure (31)-(33) with $b = 1$ is less than 0.017 % (which is negligible). This shows the efficiency of the proposed procedure to evaluate the worst case amplitude of the output over the systems in \mathcal{D}^{dyn} . For the sake of completion, let us mention that $G_{grid}^{dyn}(e^{j\omega_1 T_s}) = 1.4279 - 0.2057j$, $G_{grid}^{dyn}(e^{j\omega_2 T_s}) = 1.1002 - 4.76999j$ and $G_{grid}^{dyn}(e^{j\omega_3 T_s}) = -1.009 - 0.4841j$ (see Figure 1). Note also that, since the worst-case amplitude of $y(t, G_{grid}^{dyn})$ is larger than y_{wc}^{par} , there is thus no second-order system $G(z, \theta)$ with $\theta \in U$ that has such a frequency response at ω_i ($i = 1, 2, 3$).

We have repeated the above procedure for a number of other complex amplitude vectors \mathcal{A} and the observed conservatism for y_{wc}^{par} and y_{wc}^{dyn} (using Proposition 2 or Proposition 3) is always small or negligible.

8 Conclusions

We have developed a methodology inspired by robustness analysis to verify robust amplitude constraints. In the extended version [9] of this paper, we use this methodology for optimal experiment design. The developed framework considers the case where the identification is performed in open loop and when the considered true system has one input and one output. In future work, we will extend the framework to closed-loop identification and to multivariable systems.

References

- [1] M. Barenthin, X. Bombois, H. Hjalmarsson, and G. Scorletti. Identification for control of multivariable systems: controller validation and experiment design via LMIs. *Automatica*, 44(12):3070–3078, 2008.
- [2] P.A. Bliman. A convex approach to robust stability for linear systems with uncertain scalar parameters. *SIAM Journal on Control and Optimization*, 42(6):2016–2042, 2004.
- [3] X. Bombois, B. Anderson, and M. Gevers. Quantification of frequency domain error bounds with guaranteed confidence level in prediction error identification. *Systems and Control Letters*, 54(5):471–482, 2005.
- [4] X. Bombois, M. Gevers, and G. Scorletti. Controller validation for stability and performance based on a frequency domain uncertainty region obtained by stochastic embedding. In *CD-ROM Proc. 39th Conference on Decision and Control*, paper TuM06-5, Sydney, Australia, 2000.
- [5] X. Bombois, M. Gevers, G. Scorletti, and B.D.O. Anderson. Robustness analysis tools for an uncertainty set obtained by prediction error identification. *Automatica*, 37(10):1629–1636, 2001.
- [6] X. Bombois, H. Hjalmarsson, and G. Scorletti. Identification for robust H_2 deconvolution filtering. *Automatica*, 46(3):577–584, 2010.
- [7] X. Bombois, F. Morelli, H. Hjalmarsson, L. Bako, and K. Colin. Robust optimal identification experiment design for multisine excitation. *Automatica*, 125:109431, 2021.
- [8] X. Bombois, G. Scorletti, M. Gevers, P.M.J. Van den Hof, and R. Hildebrand. Least costly identification experiment for control. *Automatica*, 42(10):1651–1662, 2006.
- [9] X. Bombois, G. Scorletti, and G. Mercère. Optimal identification experiment design with robust output amplitude constraints. HAL-document hal-04247863, 2023, available at <https://hal.science/hal-04247863/>.
- [10] J. Gardner, M. Kusner, Z. Xu, K. Weinberger, and J. Cunningham. Bayesian optimization with inequality constraints. In *ICML*, volume 2014, pages 937–945, 2014.
- [11] K.C. Goh and M.G. Safonov. Robust analysis, sectors and quadratic functionals. In IEEE, editor, *Proc. IEEE Conf. on Decision and Control*, New Orleans, Louisiana, 1995.
- [12] G. Goodwin, M. Gevers, and B. Ninness. Quantifying the error in estimated transfer functions with application to model order selection. *IEEE Transactions on Automatic Control*, 37(7):913–928, 1992.
- [13] R. Hakvoort and P. Van den Hof. Consistent parameter bounding identification for linearly parametrized model sets. *Automatica*, 31(7):957–959, 1995.
- [14] H. Hjalmarsson. System identification of complex and structured systems. *European Journal of Control*, 15(3-4):275–310, 2009.
- [15] T. Iwasaki and S. Hara. Generalized KYP lemma: Unified frequency domain inequalities with design applications. *IEEE Transactions on Automatic Control*, 50(1):41–59, 2005.
- [16] L. Ljung. *System Identification: Theory for the User, 2nd Edition*. Prentice-Hall, Englewood Cliffs, NJ, 1999.
- [17] I.R. Manchester. Input design for system identification via convex relaxation. In *49th IEEE Conference on Decision and Control (CDC)*, pages 2041–2046. IEEE, 2010.
- [18] I.R. Manchester. Amplitude-constrained input design: Convex relaxation and application to clinical neurology. *IFAC Proceedings Volumes*, 45(16):1617–1622, 2012. 16th IFAC Symposium on System Identification.
- [19] A. Megretski and A. Rantzer. System analysis via integral quadratic constraints. *IEEE Transactions on Automatic Control*, 42:819–830, 1997.
- [20] W. Reinelt, A. Garulli, and L. Ljung. Comparing different approaches to model error modeling in robust identification. *Automatica*, 38(5):787–803, 2002.

- [21] M. G. Safonov. *Stability and Robustness of Multivariable Feedback Systems*. MIT Press, Cambridge, 1980.
- [22] K. Zhou and J. Doyle. *Essentials of Robust Control*. Prentice Hall, Upper Saddle River, New Jersey, 1998.

A Matrices M_u , M_y^{par} and M_y^{dyn}

Let us first note that the complex vector $\tilde{U}(\tau)$ can be expressed as the following LFT in τI_{α_L} :

$$\tilde{U}(\tau) = (\tau I_{\alpha_L}) \star \left(\begin{array}{c|c} M_{11,\mathcal{U}} & M_{12,\mathcal{U}} \\ \hline M_{21,\mathcal{U}} & 0 \end{array} \right) \quad (\text{A.1})$$

with $M_{12,\mathcal{U}} = (1, 0, \dots, 0)^T$, $M_{21,\mathcal{U}}$ a matrix whose entries are equal to zero except the entries (i, α_i) for $i = 1, \dots, L$ which are equal to one, and with $M_{11,\mathcal{U}}$ a matrix of dimension $\alpha_L \times \alpha_L$ given by

$$M_{11,\mathcal{U}} = \begin{pmatrix} 0 & 0 \\ I_{\alpha_{L-1}} & 0 \end{pmatrix}.$$

Consequently, we obtain the following LFT for $x_u(\tau)$

$$x_u(\tau) = \mathcal{A}^T \tilde{U}(\tau) = (\tau I_{\alpha_L}) \star \underbrace{\left(\begin{array}{c|c} M_{11,\mathcal{U}} & M_{12,\mathcal{U}} \\ \hline \mathcal{A}^T M_{21,\mathcal{U}} & 0 \end{array} \right)}_{=M_u},$$

from which the matrix M_u in (18) can be determined. Let us now turn to the LFT representation of $x_y^{par}(\tau, \delta)$. Let us first note that, for an arbitrary frequency ω , the frequency response $G(e^{j\omega T_s}, \theta)$ of an arbitrary plant in \mathcal{D}^{par} (see (12)) can be written as the following LFT in θ :

$$G(e^{j\omega T_s}, \theta) = (\theta) \star \left(\begin{array}{c|c} -Z_D(e^{j\omega T_s}) & 1 \\ \hline Z_N(e^{j\omega T_s}) & 0 \end{array} \right).$$

Applying the linear change of variable $\theta = \hat{\theta} + V\delta$, we obtain the LFT of $\tilde{G}(e^{j\omega T_s}, \delta) = G(e^{j\omega T_s}, \hat{\theta} + V\delta)$:

$$\tilde{G}(e^{j\omega T_s}, \delta) = (\delta) \star \left(\begin{array}{c|c} M_{11,par}(\omega) & M_{12,par}(\omega) \\ \hline M_{21,par}(\omega) & M_{22,par}(\omega) \end{array} \right),$$

with $M_{11,par}(\omega) = -\sigma(e^{j\omega T_s})Z_D(e^{j\omega T_s})V$, $M_{12,par}(\omega) = \sigma(e^{j\omega T_s})$, $M_{22,par}(\omega) = \zeta(e^{j\omega T_s})\sigma(e^{j\omega T_s})$, $M_{21,par}(\omega) = (Z_N(e^{j\omega T_s}) - \zeta(e^{j\omega T_s})\sigma(e^{j\omega T_s})Z_D(e^{j\omega T_s}))V$, and with $\sigma(e^{j\omega T_s}) = (1 + Z_D(e^{j\omega T_s})\hat{\theta})^{-1}$ and $\zeta(e^{j\omega T_s}) = Z_N(e^{j\omega T_s})\hat{\theta}$. Considering the above LFT for each frequency ω_i ($i = 1, \dots, L$) present in the multisine (1), we see that the matrix $diag(\tilde{G}(e^{j\omega_1 T_s}, \delta), \dots, \tilde{G}(e^{j\omega_L T_s}, \delta))$ in the expression (15) for $x_y^{par}(\tau, \delta)$ is equal to:

$$(I_L \otimes \delta) \star \left(\begin{array}{c|c} \bar{M}_{11,par} & \bar{M}_{12,par} \\ \hline \bar{M}_{21,par} & \bar{M}_{22,par} \end{array} \right),$$

with $\bar{M}_{mn,par} = bdiag(M_{mn,par}(\omega_1), \dots, M_{mn,par}(\omega_L))$ ($m = 1, 2, n = 1, 2$).

Using this expression and the LFT (A.1) for $\tilde{U}(\tau)$, $x_y^{par}(\tau, \delta)$ (see (15)) is then given by the LFT in (18) with

$$M_y^{par} = \left(\begin{array}{cc|c} M_{11,\mathcal{U}} & 0 & M_{12,\mathcal{U}} \\ \hline \bar{M}_{12,par} M_{21,\mathcal{U}} & \bar{M}_{11,par} & 0 \\ \mathcal{A}^T \bar{M}_{22,par} M_{21,\mathcal{U}} & \mathcal{A}^T \bar{M}_{21,par} & 0 \end{array} \right).$$

Let us now turn to the LFT representation of $x_y^{dyn}(\tau, \delta(\omega_1), \dots, \delta(\omega_L))$. Let us first note that, for an arbitrary frequency ω , the frequency response $G(e^{j\omega T_s})$ of an arbitrary plant in \mathcal{D}^{dyn} (see (13)) can be written as the following LFT in $\delta(\omega)$:

$$G(e^{j\omega T_s}) = (\delta(\omega)) \star \left(\begin{array}{c|c} 0 & 1 \\ \hline v_P^T(\omega) & \hat{G}(e^{j\omega T_s}) \end{array} \right). \quad (\text{A.2})$$

Considering the above LFT for each frequency ω_i ($i = 1, \dots, L$) present in the multisine (1), we see that the matrix $diag(G(\delta(\omega_1)), \dots, G(\delta(\omega_L)))$ in the expression (17) for $x_y^{dyn}(\tau, \delta(\omega_1), \dots, \delta(\omega_L))$ is equal to:

$$(diag(\delta(\omega_1), \dots, \delta(\omega_L))) \star \left(\begin{array}{c|c} 0 & I_L \\ \hline \bar{M}_{21,dyn} & \bar{M}_{22,dyn} \end{array} \right),$$

with $\bar{M}_{21,dyn} = bdiag(v_P^T(\omega_1), \dots, v_P^T(\omega_L))$ and $\bar{M}_{22,dyn} = diag(\hat{G}(e^{j\omega_1 T_s}), \dots, \hat{G}(e^{j\omega_L T_s}))$. Using this expression and the LFT (A.1) for $\tilde{U}(\tau)$, $x_y^{dyn}(\tau, \delta(\omega_1), \dots, \delta(\omega_L))$ (see (17)) is then given by the LFT in (18) with

$$M_y^{dyn} = \left(\begin{array}{cc|c} M_{11,\mathcal{U}} & 0 & M_{12,\mathcal{U}} \\ M_{21,\mathcal{U}} & 0 & 0 \\ \hline \mathcal{A}^T \bar{M}_{22,dyn} M_{21,\mathcal{U}} & \mathcal{A}^T \bar{M}_{21,dyn} & 0 \end{array} \right).$$

B Structure of \tilde{B} , \tilde{D} , \tilde{P} , \tilde{Z} in Proposition 5

As shown in [1], the real matrices \tilde{B} and \tilde{D} in the expression of $\Sigma_{m,n}$ have the following structures:

$$\tilde{B} = \begin{pmatrix} 0 & K_{12} & \dots & K_{1m} \\ -K_{12} & 0 & \dots & \vdots \\ \vdots & & \ddots & K_{(m-1)m} \\ -K_{1m} & \dots & -K_{(m-1)m} & 0 \end{pmatrix}$$

$$\tilde{D} = \begin{pmatrix} R_{11} & R_{12} & \dots & R_{1m} \\ R_{12} & R_{22} & \dots & R_{2m} \\ \vdots & & \ddots & \vdots \\ R_{1m} & R_{2m} & \dots & R_{mm} \end{pmatrix},$$

with the constraints that all blocks K_{il} (resp. R_{il}) satisfy $K_{il} = -K_{il}^T \in \mathbb{R}^{n \times n}$ (resp. $R_{il} = -R_{il}^T \in \mathbb{R}^{n \times n}$). The matrix \tilde{P} (resp. \tilde{Z}) has a similar structure as \tilde{B} (resp. \tilde{D}), but with the skew-symmetric blocks replaced by row vectors of dimension n [1].

C Proof of Proposition 6

Before giving the proof, let us present the following result which is a particular case of the generalized KYP lemma [15].

Lemma 1 ([15]) *Consider a matrix $\mathcal{F}(\tau)$ which depends on a complex scalar variable τ that lies in the set \mathcal{T} defined in (11). Assume that $\mathcal{F}(\tau)$ can be written as an LFT in τI_α and that this LFT is minimal (i.e., we cannot write $\mathcal{F}(\tau)$ as an LFT in $\tau I_{\tilde{\alpha}}$ with $\tilde{\alpha} < \alpha$). We thus have:*

$$\mathcal{F}(\tau) = (\tau I_\alpha) \star \left(\begin{array}{c|c} \mathcal{F}_{11} & \mathcal{F}_{12} \\ \hline \mathcal{F}_{21} & \mathcal{F}_{22} \end{array} \right) \quad (\text{C.1})$$

where \mathcal{F}_{11} is a matrix of dimension $\alpha \times \alpha$. Consider finally a Hermitian matrix Ω of appropriate dimension. Then, $\mathcal{F}^*(\tau)\Omega\mathcal{F}(\tau) \leq 0$ for all $\tau \in \mathcal{T}$ is equivalent to the existence of $\Xi_\alpha \in \Xi_\alpha$ (see Proposition 4) such that:

$$\begin{aligned} & \left(\begin{array}{cc} I & 0 \\ \mathcal{F}_{11} & \mathcal{F}_{12} \end{array} \right)^* \Pi_\alpha \left(\begin{array}{cc} I & 0 \\ \mathcal{F}_{11} & \mathcal{F}_{12} \end{array} \right) + \dots \\ & \dots + \left(\mathcal{F}_{21} \ \mathcal{F}_{22} \right)^* \Omega \left(\mathcal{F}_{21} \ \mathcal{F}_{22} \right) \leq 0. \end{aligned} \quad (\text{C.2})$$

■

The proof of Proposition 6 is then rather straightforward. When we perform the product $\Psi_{\Sigma_{m,n}}^*(\tau)\mathcal{P}_{\Sigma_{m,n}}\Psi_{\Sigma_{m,n}}(\tau)$, we indeed obtain a matrix having the structure (38) for any value of $\tau \in \mathcal{T}$. More precisely, the matrix Q in (38) is given by $(\mathcal{N}^*(\tau) \otimes I_m)\Lambda(\mathcal{N}(\tau) \otimes I_m) = Q_0 + Q_1\tau + Q_1^*\tau^* + \dots + Q_b\tau^b + Q_b^*(\tau^b)^*$. It is clear that this matrix is Hermitian for all $\tau \in \mathcal{T}$. Moreover, the LMI condition (41) ensures that this Hermitian matrix is also positive semi-definite for all $\tau \in \mathcal{T}$. The latter is a consequence of Lemma 1 with $\mathcal{F}(\tau) = \mathcal{N}(\tau) \otimes I_m$, $\alpha = bm$ and $\Omega = -\Lambda$. Since $\mathcal{N}(\tau) = (\tau I_b) \star \tilde{\mathcal{N}}$ (see (39)), we have indeed that:

$$\mathcal{F}(\tau) = \mathcal{N}(\tau) \otimes I_m = (\tau I_{bm}) \star \left(\begin{array}{c|c} \tilde{\mathcal{N}}_{m,11} & \tilde{\mathcal{N}}_{m,12} \\ \hline \tilde{\mathcal{N}}_{m,21} & \tilde{\mathcal{N}}_{m,22} \end{array} \right)$$

with $\tilde{\mathcal{N}}_{m,11}$, $\tilde{\mathcal{N}}_{m,12}$, $\tilde{\mathcal{N}}_{m,21}$ and $\tilde{\mathcal{N}}_{m,22}$ as defined in the statement of Proposition 6.

Then, when we perform the product $\Psi_{\Sigma_{m,n}}^*(\tau)\mathcal{P}_{\Sigma_{m,n}}\Psi_{\Sigma_{m,n}}(\tau)$, the matrix $j\tilde{D}$ in (38) is given by

$$j\tilde{D} = j\tilde{D}_0 + (0, \tilde{D}_1, \dots, \tilde{D}_b) (\mathcal{N} \otimes I_{mn}) + (\mathcal{N}^* \otimes I_{mn}) \begin{pmatrix} 0 \\ \tilde{D}_1^T \\ \dots \\ \tilde{D}_b^T \end{pmatrix}$$

The right hand side of this expression is equal to $j\tilde{D}_0 + \tilde{D}_1(\tau - \tau^*) + \dots + \tilde{D}_b(\tau^b - (\tau^b)^*)$ since $\tilde{D}_i = -\tilde{D}_i^T$ ($i = 1, \dots, b$). It is clear that this expression has indeed the desired structure since $\tau^i - (\tau^i)^*$ ($i = 1, \dots, b$) is an imaginary number for all $\tau \in \mathcal{T}$. In $\Psi_{\Sigma_{m,n}}^*(\tau)\mathcal{P}_{\Sigma_{m,n}}\Psi_{\Sigma_{m,n}}(\tau)$, the matrix $j\tilde{Z}$ in (38) is given by

$$j\tilde{Z} = j\tilde{Z}_0 + (0, \tilde{Z}_1, \dots, \tilde{Z}_b) (\mathcal{N} \otimes I_{mn}) - (\mathcal{N}^* \otimes I_m) \begin{pmatrix} 0 \\ \tilde{Z}_1 \\ \dots \\ \tilde{Z}_b \end{pmatrix}$$

The right hand side of this expression is equal to $j\tilde{Z}_0 + \tilde{Z}_1(\tau - \tau^*) + \dots + \tilde{Z}_b(\tau^b - (\tau^b)^*)$ which has thus also the desired structure. Following the same procedure, the matrix \tilde{B} in (38) is given by $2\tilde{B}_0 + \tilde{B}_1(\tau + \tau^*) + \dots + \tilde{B}_b(\tau^b + (\tau^b)^*)$ since $\tilde{B}_i = \tilde{B}_i^T$ ($i = 1, \dots, b$) while the matrix \tilde{P} in (38) is given by $2\tilde{P}_0 + \tilde{P}_1(\tau + \tau^*) + \dots + \tilde{P}_b(\tau^b + (\tau^b)^*)$. These expressions have the desired structure since $\tau^i + (\tau^i)^*$ ($i = 1, \dots, b$) is a real number for all $\tau \in \mathcal{T}$.

Remark. In Proposition 1 of [6], we proposed a less general parametrization for $\mathcal{P}_{\Sigma_{m,n}}$ where the matrices Q_i were restricted to be real matrices, the factorizations of $j\tilde{D}$ was reduced to $\tilde{D}_1(\tau - \tau^*) + \dots + \tilde{D}_b(\tau^b - (\tau^b)^*)$ and the one of $j\tilde{Z}$ to $\tilde{Z}_1(\tau - \tau^*) + \dots + \tilde{Z}_b(\tau^b - (\tau^b)^*)$.

D Proof of Proposition 7

Observe that the LMI (23) with $r = 0$, $\mathbf{\Pi}_0 = \Xi_{\alpha_L}$ and with M_x, M_0 (see (20)) obtained from the decomposition of M_u is equivalent to (C.2) with $\alpha = \alpha_L$,

$$\Omega = \begin{pmatrix} -\gamma & 0.5 \\ 0.5 & 0 \end{pmatrix}, \quad (\mathcal{F}_{11} \ \mathcal{F}_{12}) = M_0 \quad \text{and} \quad (\mathcal{F}_{21} \ \mathcal{F}_{22}) =$$

$[Z_x^T \ M_x^T]^T$. The matrix $\mathcal{F}(\tau)$ in (C.1) is thus $\mathcal{F}(\tau) \triangleq (1 \ x_u(\tau))^T$. Using Lemma 1 in Appendix C, we thus have that the LMI (23) is equivalent to

$$\mathcal{F}^*(\tau)\Omega\mathcal{F}(\tau) = \text{Re}(x_u(\tau)) - \gamma \leq 0 \quad \forall \tau \in \mathcal{T}.$$

A similar reasoning shows that (24) is equivalent to $-\gamma \leq \text{Re}(x_u(\tau))$ for all $\tau \in \mathcal{T}$. Combining these two facts shows that the LMI optimization problem (22)-(24) yields a solution γ_{opt} which is equal to u_{wc} .